Benzodiazepine treatment induces subtype-specific changes in $GABA_A$ receptor trafficking and decreases synaptic inhibition

Tija C. Jacob[a], Guido Michels[b], Liliya Silayeva[c], Julia Haydon[c], Francesca Succol[d], and Stephen J. Moss[c,1]

[a]Department of Pharmacology and Chemical Biology, University of Pittsburgh School of Medicine, Pittsburgh, PA 15261; [b]Internal Medicine Clinic III, University of Cologne, 50937 Cologne, Germany; [c]Department of Neuroscience, Tufts University School of Medicine, Boston, MA 02111; and [d]Neuroscience and Brain Technology, The Italian Institute of Technology, 16163 Genoa, Italy

Edited by Richard L. Huganir, The Johns Hopkins University School of Medicine, Baltimore, MD, and approved September 28, 2012 (received for review March 30, 2012)

Benzodiazepines potentiate γ-aminobutyric acid type A receptor ($GABA_AR$) activity and are widely prescribed to treat anxiety, insomnia, and seizure disorders. Unfortunately, clinical use of benzodiazepines (BZs) is severely limited by tolerance. The mechanisms leading to BZ tolerance are unknown. BZs bind at the interface between an α and γ subunit of $GABA_ARs$, preferentially enhancing synaptic receptors largely composed of α(1–3, 5), β3, and γ2 subunits. Using confocal imaging and patch-clamp approaches, we show that treatment with the BZ flurazepam decreases $GABA_AR$ surface levels and the efficacy of neuronal inhibition in hippocampal neurons. A dramatic decrease in surface and total levels of α2 subunit-containing $GABA_ARs$ occurred within 24 h of flurazepam treatment, whereas $GABA_ARs$ incorporating α1 subunits showed little alteration. The $GABA_AR$ surface depletion could be reversed by treatment with the BZ antagonist Ro 15-1788. Coincident with decreased $GABA_AR$ surface levels, flurazepam treatment reduced miniature inhibitory postsynaptic current amplitude, which returned to control levels with acute Ro 15-1788 treatment. $GABA_AR$ endocytosis and insertion rates were unchanged by flurazepam treatment. Treatment with leupeptin restored flurazepam lowered receptor surface levels, strongly suggesting that flurazepam increases lysosomal degradation of $GABA_ARs$. Together, these data suggest that flurazepam exposure enhances degradation of α2 subunit-containing $GABA_ARs$ after their removal from the plasma membrane, leading to a reduction in inhibitory synapse size and number along with a decrease in the efficacy of synaptic inhibition. These reported subtype-specific changes in $GABA_AR$ trafficking provide significant mechanistic insight into the initial neuroadaptive responses occurring with BZ treatment.

GABAergic | diazepam | lysosome

$GABA_A$ receptors ($GABA_ARs$) are Cl^--selective ligand-gated ion channels that mediate fast inhibition in the CNS and are important targets for benzodiazepines (BZs), drugs used to treat anxiety, insomnia, and seizure disorders and as adjunct treatments in both depression and schizophrenia. BZs enhance chloride ion conductance primarily by increasing the frequency of receptor channel opening and slowing the decay of miniature inhibitory postsynaptic currents (mIPSCs) (1–3). Structurally, $GABA_ARs$ are pentameric heterooligomers that can be constructed from eight subunit classes with multiple members: α(1–6), β(1–3), γ(1–3), δ, ε, θ, π, and ρ(1–3) (4, 5). Molecular and genetic studies have revealed that synaptic BZ-sensitive $GABA_AR$ subtypes are composed of α(1–3, 5), β, and γ2 subunits, whereas $GABA_AR$ subtypes composed of α4/6, β, and δ subunits form a specialized population of extrasynaptic receptors that mediate tonic inhibition but are insensitive to modulation by BZ (reviewed in ref. 6).

BZs are highly prescribed and of major clinical significance; however, the development of tolerance restricts their usefulness and has prompted research on the mechanism for several decades. Chronic BZ treatment results in allosteric uncoupling of the GABA and BZ binding sites, suggesting changes in receptor subunit composition and/or receptor function (reviewed in ref. 7). Chronic dosing of animals with BZ leads to a reduction in $GABA_AR$ synaptic inhibition (8–10) and produces diverse changes in $GABA_AR$ transcripts across the brain (7). Direct comparison and interpretation of these and other studies assessing mRNA levels has been challenging due to differences in treatment paradigm (time and dose), brain regions assessed, and the BZ ligand used. Radioligand binding studies have reported mixed results, ranging from decreases to no change in CNS BZ binding sites, likely due to methodological limitations in assessing subtype-specific $GABA_AR$ changes.

The surface level of postsynaptic $GABA_ARs$ is a critical determinant of the strength of synaptic inhibition and is largely dependent on regulated trafficking steps to and from the plasma membrane, including receptor insertion, diffusion within the membrane, receptor removal, and degradation (11). Biochemical studies show that at least 40% of the total cell surface population of $GABA_ARs$ is internalized within 1 h (12). Endocytosed receptors are either rapidly recycled back to the surface for reinsertion or targeted for lysosomal degradation. In addition, $GABA_AR$ surface levels can be regulated by controlling the receptor pool available for insertion, the size of which is primarily determined by endoplasmic reticulum-associated degradation (13). Modulation of $GABA_AR$ turnover has been widely invoked to explain the development of tolerance to BZs. However, it remains to be determined whether exposure of neurons to BZs modifies the surface stability of $GABA_ARs$ or the efficacy of synaptic inhibition.

We demonstrate here that 24-h treatment with the BZ flurazepam (Flz) dramatically decreases α2 subunit-containing $GABA_AR$ surface and total levels without comparable changes in levels of the α1 subunit. BZ treatment does not appear to alter receptor insertion and removal rates. However, treatment with leupeptin, an inhibitor of lysosomal proteolysis, restores BZ-lowered $GABA_AR$ levels. The observed decrease in $GABA_AR$ surface levels and synaptic inhibition occurs in a BZ binding site-dependent fashion because these alterations can be rescued by treatment with the BZ antagonist Ro 15-1788. Together, these data suggest that Flz exposure enhances degradation of α2-subtype $GABA_ARs$ after endocytosis, leading to a reduction in inhibitory synapse size and number along with a decrease in the efficacy of synaptic inhibition.

Results

Acute BZ Treatment Decreases $GABA_AR$ Surface Levels. To directly address the role of BZ in regulating $GABA_AR$ surface levels,

Author contributions: T.C.J., G.M., and S.J.M. designed research; T.C.J., G.M., L.S., J.H., and F.S. performed research; T.C.J. contributed new reagents/analytic tools; T.C.J., G.M., and L.S. analyzed data; and T.C.J. wrote the paper.

The authors declare no conflict of interest.

This article is a PNAS Direct Submission.

[1]To whom correspondence should be addressed. E-mail: stephen.moss@tufts.edu.

This article contains supporting information online at www.pnas.org/lookup/suppl/doi:10.1073/pnas.1204994109/-/DCSupplemental.

we performed live-imaging studies of pH-sensitive GFP-tagged $GABA_AR$ α1 ($α1^{pHGFP}$) and α2 ($α2^{pHGFP}$) subunits in hippocampal neurons. The addition of this reporter to receptor subunits is functionally silent and allows the specific visualization of surface $GABA_AR$ populations in living neurons (14, 15). Furthermore, BZ potentiation of GABA-induced currents is equivalent in HEK-293 cells expressing these tagged or untagged $GABA_AR$ α subunits cotransfected with β3γ2 subunits (Table S1). We measured the surface levels of BZ-sensitive $GABA_ARs$ containing $α1^{pHGFP}$ or $α2^{pHGFP}$ subunits with 24-h 250 nM Flz or control treatment with live confocal microscopy at 37 °C in Hepes-buffered saline (HBS) (pH 7.4). Twenty-four-hour Flz treatment dramatically decreased α2 subunit-containing $GABA_AR$ surface levels on three measured parameters, expressed as percentage control: surface cluster area (65.0 ± 2.8%), average cluster fluorescence intensity (87.1 ± 2.2%), and density (58.7 ± 17%) (Fig. 1 *A* and *B*). Minor changes were observed in α1-subtype $GABA_AR$ surface levels, with a significant decrease only in average cluster fluorescence intensity (96.5 ± 1.3%) (Fig. 1 *A* and *B*).

BZ Treatment Alters Total $GABA_AR$ Levels. Because these initial studies revealed a major decrease in α2-containing $GABA_AR$ surface levels and a minimal change in α1-containing $GABA_AR$ surface levels with 24-h BZ treatment, subsequent experiments focused on the α2 subunit. We tested whether total BZ-sensitive $GABA_AR$ protein levels were altered in Flz-treated neurons. To do so, we visualized pHGFP-tagged $GABA_ARs$ resident inside the neurons by equalizing the pH of all intracellular compartments to pH 7.4 with a brief perfusion of NH_4Cl in HBS (NH_4Cl in place of equimolar NaCl) (Fig. 1*C*). This experiment revealed that total α2-subunit levels were decreased dramatically, with the ratio of total/surface α2 being approximately threefold lower following BZ treatment (control total/surface ratio, 277 ± 36%, normalized to Flz total/surface ratio) (Fig. 1 *C* and *D*).

Decreases in $GABA_AR$ Surface Levels Occur via a BZ Binding Site-Dependent Mechanism. Next, we tested whether the decrease in α2-subtype $GABA_AR$ surface levels was specifically induced by BZ binding. Live-cell confocal microscopy was used to measure $α2^{pHGFP}$ fluorescence in neurons with 24-h Flz or control treatment followed by an acute 1-h treatment with 5 μM BZ antagonist Ro 15-1788 (Fig. 2 *A* and *B*). One-hour treatment with Ro 15-1788 restored the BZ-lowered $GABA_AR$ surface levels to control levels (cluster area in $μm^2$: control, 0.232 ± 0.008; Flz, 0.184 ± 0.006; Flz plus Ro 15-1788, 0.216 ± 0.010; and total cluster fluorescence expressed as % control: control, 101.4 ± 5.4; Flz, 73.4 ± 3.6; Flz plus Ro 15-1788, 96.5 ± 5.3) (Fig. 2*B*). Control neurons treated with Ro 15-1788 showed no significant change on any measured parameter (control plus Ro 15-1788 cluster area in $μm^2$, 0.242 ± 0.006; and total cluster fluorescence expressed as % control, 104.9 ± 5.4) (Fig. 2*B*). Interestingly, the BZ antagonist did not significantly increase $GABA_AR$ surface cluster density in Flz neurons, suggesting that existing inhibitory synapses are preferentially restored (clusters per 20 μm: control, 6.8 ± 2.2; Flz, 5.4 ± 1.2; control plus Ro 15-1788, 6.9 ± 1.8; Flz plus Ro 15-1788, 5.4 ± 1.6).

Prolonged Exposure of Neurons to BZ Reduces mIPSCs. Having determined that surface and total levels of α2-subtype $GABA_ARs$ are decreased by 24-h BZ exposure, we next measured the functional effects of prolonged BZ treatment on GABAergic inhibition. It is well established that rapid application of BZ to neurons enhances $GABA_AR$ function due to an increase in the probability of channel opening. Although this results in an increased amplitude and slowed decay of mIPSCs (16, 17), the effects of prolonged initial treatment remain to be addressed. We directly compared the properties of mIPSCs in control neurons and those pretreated with Flz for 24 h before recording.

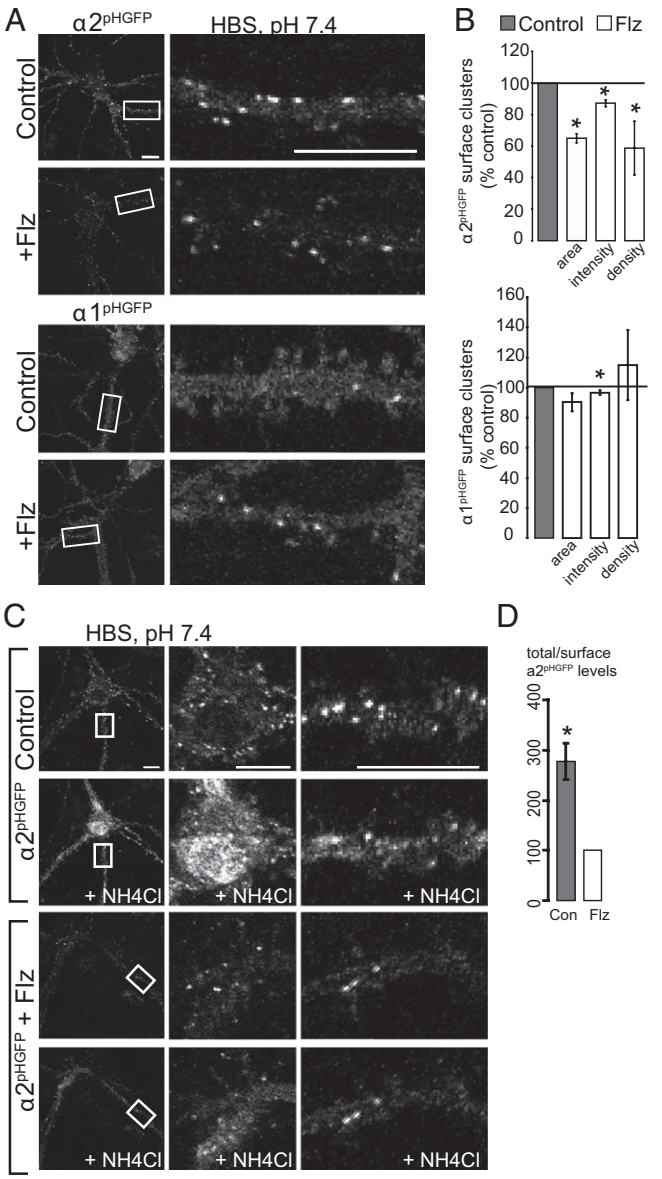

Fig. 1. Acute BZ treatment decreases surface and total $GABA_AR$ levels. (*A*) Neurons expressing $α2^{pHGFP}$ or $α1^{pHGFP}$ $GABA_AR$ subunits were incubated with or without 250 nM flurazepam (Flz) for 24 h followed by live confocal microscopy experiments (37 °C in HBS). (*Right*) Enlargements of dendrites in boxed areas. (*B*) Mean ± SEM cluster size, fluorescence intensity, and density of surface $GABA_AR$ clusters normalized to control (*significantly different from control, $P < 0.05$, *t* test; $n = 15–20$ neurons, 3 independent cultures). (*C*) Neurons were perfused at a rate of 1 mL/min with pH 7.4 HBS followed by HBS with 50 mM NH_4Cl ($+NH_4Cl$) to collapse the intracellular pH gradients and reveal intracellular $GABA_AR$. The center panels are enlargement of cell bodies, and the right panels are dendrites in boxed areas. (*D*) The ratio of $α2^{pHGFP}$ total/surface levels was normalized to Flz-treated neurons (*$P < 0.05$, *t* test; $n = 6–8$ neurons per culture, 3 independent cultures; error bars represent ±SEM). (Scale bars, 10 μm.)

BZ treatment resulted in a significant decrease in mIPSC amplitude from 52.5 ± 2.7 in control neurons to 42.2 ± 2.4 pA in those exposed to Flz for 24 h. In contrast mIPSC frequency (in Hz: control, 1.08 ± 0.34; Flz, 0.69 ± 0.12; Flz plus Ro 15-1788, 0.68 ± 0.10), 10–90% rise time (in ms: control, 1.46 ± 0.08; Flz, 1.68 ± 0.11; Flz plus Ro 15-1788, 1.59 ± 0.11), and decay times (in ms: control, 43.4 ± 1.19; Flz, 47.6 ± 2.34; Flz plus Ro 15-1788, 46.1 ± 1.66) were unaffected by prolonged exposure to BZ (Fig.

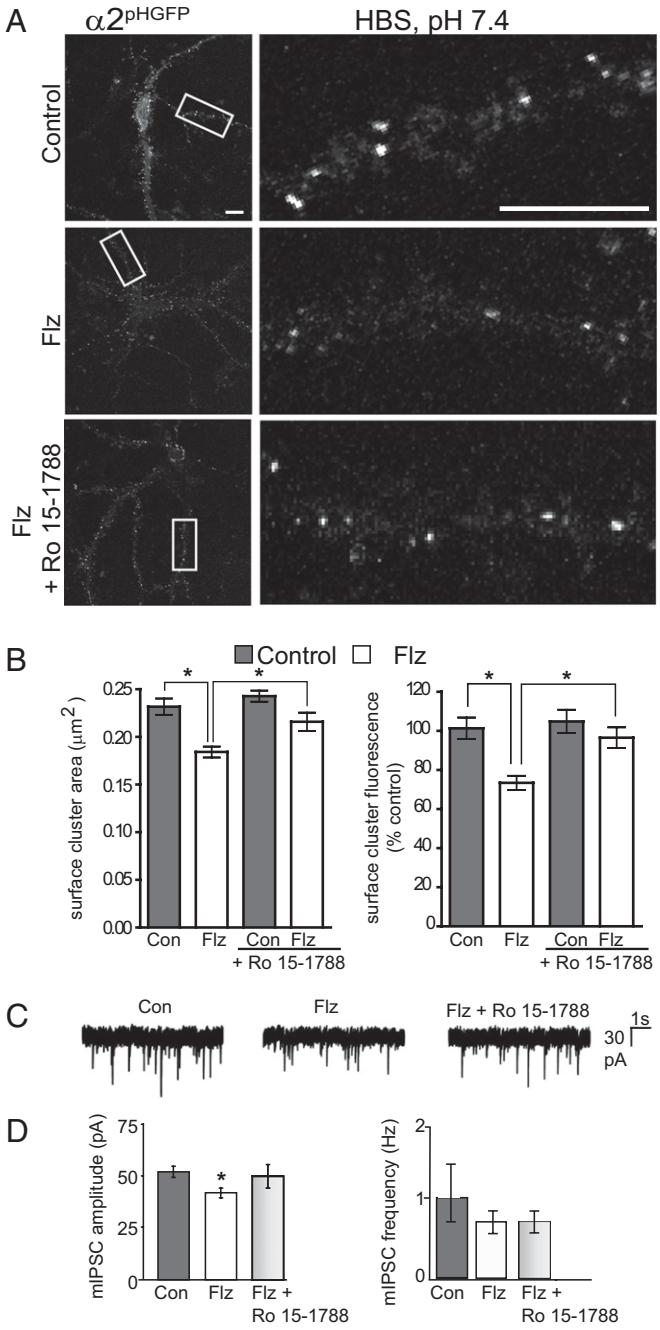

Fig. 2. Decreases in $GABA_AR$ surface levels and GABAergic mIPSC amplitude occur via a BZ binding site-dependent mechanism. (*A*) Neurons expressing $\alpha2^{pHGFP}$ were incubated with or without 250 nM Flz for 24 h and then treated for 1 h with 5 μM Ro 15-1788 (BZ antagonist) immediately before live imaging confocal microscopy experiments (37 °C in HBS). (*Right*) Enlargements of dendrites in boxed areas. (Scale bars, 10 μm.) (*B*) Surface cluster histograms showing mean area and cumulative $\alpha2^{pHGFP}$ fluorescence in neurons with 24-h control (Con) or 250 nM Flz conditions with or without 1-h 5 μM Ro 15-1788 treatment (*$P < 0.05$, one-way ANOVA analysis and Bonferroni's multiple-comparison test; 22–30 neurons; $n = 3$ cultures; error bars represent ± SEM). (*C*) Sample traces of mIPSCs in control (Con) neurons and those treated with 250 nM Flz for 24 h with or without 1-h 5 μM Ro 15-1788 treatment. (*D*) Bar graph of the mean ± SEM mIPSC amplitudes and frequency (*$P < 0.05$, Kolmogorov–Smirnov test; $n = 7$–10 cells for each condition).

2 *C* and *D*). One-hour treatment with the BZ antagonist Ro 15-1788 restored mIPSC amplitude to control levels (50.2 ± 5.7 pA). The rapid timescale of Ro 15-1788 action is consistent with BZ-induced changes affecting receptor trafficking pathways rather than protein synthesis. Furthermore, these results are consistent with the efficacy of Ro 15-1788 reversing in vitro and in vivo BZ tolerance (18).

BZ Treatment Does Not Alter the Rates of $GABA_AR$ Insertion and Removal. It is increasingly apparent that $GABA_ARs$ on the surface of neurons are dynamic entities that undergo regulated exocytosis and constitutive clathrin-mediated, dynamin-dependent endocytosis. Changes in the rates of exocytosis or endocytosis could clearly contribute to a mechanism for BZ-dependent alteration of $GABA_AR$ surface levels. To measure the insertion and removal rate of α2-containing $GABA_ARs$, we generated a construct with a bungarotoxin (Bgt) binding site (BBS) and pHGFP encoded in the N terminus of the $GABA_AR$ subunit ($\alpha2^{pHBBS}$). The BBS allows the monitoring of receptor insertion and endocytosis with application of exogenous fluorescent Bgt and does not modify the assembly or functional properties of $GABA_ARs$ (13, 19, 20). Bgt insertion assays were performed on $\alpha2^{pHBBS}$-expressing neurons undergoing control and 24-h 250 nM Flz treatments. Neurons were first incubated with unlabeled Bgt at 15 °C to block existing surface $GABA_AR$ receptor populations, and then washed followed by incubation with Alexa 594-conjugated Bgt at 37 °C to label newly inserted receptors. At 5, 10, and 15 min, samples were removed, fixed, and permeabilized, and the total receptor population was labeled with anti-GFP antibody. Quantification and analysis of surface receptor signal in control and Flz-treated neurons produced similar results to live imaging (Fig. 1), with BZ-treated neurons showing a decrease to 51.59 ± 7.3% control (Fig. 3 *A* and *B*). The fluorescence intensity of newly inserted $\alpha2^{pHBBS}$ over a 15-min time course (normalized to the initial fluorescence value of each treatment) was compared in control and Flz conditions (Fig. 3 *A* and *C*), revealing that the rate of $GABA_AR$ insertion was not significantly changed by BZ treatment (Bgt fluorescence count at $t = 10$ min: control, 364.5 ± 112.1%; Flz, 305.3.1 ± 12.2; and at $t = 15$ min: control, 437 ± 129.5%; Flz, 389 ± 22.6%).

We next measured the rate of endocytosis in control versus Flz-treated neurons expressing $\alpha2^{pHBBS}$ using an established fluorescent endocytosis assay (19). Surface $GABA_AR$ were live-labeled with Alexa594::Bgt for 5 min at 37 °C, followed by washing to remove unbound Alexa594::Bgt, and then incubated at 37 °C. At $t = 0$, 7.5, and 15 min, neurons were removed from the incubator and fixed. Total receptor number was visualized by permeabilization and staining with anti-GFP antibody. Quantification of confocal microscopy images showed loss of Alexa594::Bgt fluorescence over time with endocytosis of surface $GABA_AR$ (Fig. 4 *A* and *B*). The Alexa594::Bgt total fluorescence count for control and Flz-treated neurons at each time point was compared with the signal at 0 time, set to a value of 100% (Fig. 4*B*). Analysis of the endocytosis assay time course indicated that the rate of $GABA_AR$ endocytosis was also not changed by BZ treatment (remaining surface Bgt fluorescence: at $t = 7.5$ min, control, 30.3 ± 8.4%, and Flz, 26.7 ± 8.4%, and at $t = 15$ min, control, 10.0 ± 5.3%; Flz, 20.7 ± 3.9%). The lack of change in exocytosis and endocytosis rates, combined with the observed dramatic decrease in total $GABA_AR$ levels, suggested that BZ treatment promotes $GABA_AR$ degradation, likely through increased lysosomal degradation of endocytosed receptors or increased endoplasmic reticulum-associated protein degradation via the proteasome.

$GABA_AR$ Surface Levels Are Restored in BZ-Treated Neurons by Leupeptin Treatment. Cell surface $GABA_ARs$ undergo constitutive endocytosis and can be recycled or targeted for degradation in the lysosome (11). We next analyzed the role of lysosomal degradation in the decrease in surface and total $GABA_AR$ levels observed with BZ exposure. Neurons were treated with or without 250 nM Flz for 24 h followed by control or 2-h 200-μM treatment with the lysosomal protease inhibitor leupeptin. Live confocal

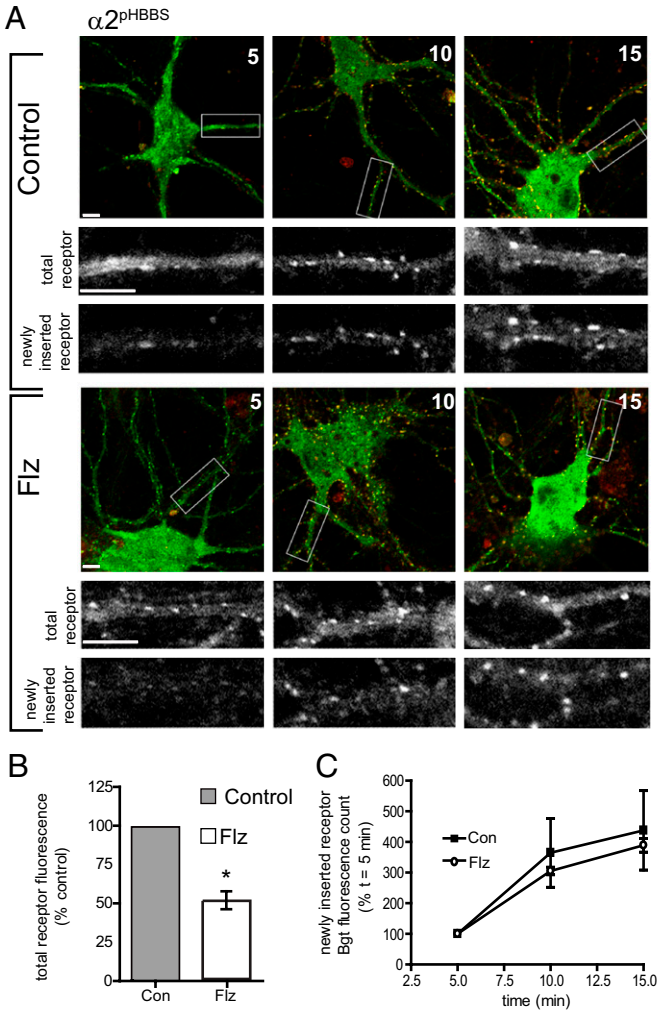

Fig. 3. BZ treatment does not alter the insertion rate of α2 subunit-containing $GABA_AR$. (*A*) Confocal imaging of $GABA_AR$ insertion in control and Flz-treated neurons. Neurons expressing $\alpha2^{pHBBS}$ were treated with or without 250 nM Flz for 24 h, and then incubated with Alexa594::Bgt (red) at 37 °C for 5, 10, and 15 min to label newly inserted $GABA_AR$, followed by fixation. Total receptor number was determined by permeabilization and staining with anti-GFP antibody (green). Panels below are enlargements of boxed dendrites. (Scale bars, 10 μm.) (*B*) Analysis of total receptor signal in control and Flz-treated $\alpha2^{pHBBS}$ neurons. (*$P < 0.01$, paired *t* test; 10–12 neurons per condition for each culture, $n = 4$ cultures; error bars represent ± SEM). (*C*) Graph shows Alexa594::Bgt fluorescence intensity of newly inserted $\alpha2^{pHBBS}$ over time in control (Con) or Flz conditions (normalized to initial fluorescence count at 5 min) (10–12 neurons per condition for each culture; $n = 4$ cultures; error bars represent ±SEM).

microscopy experiments were used to measure surface $\alpha2^{pHGFP}$-subtype $GABA_AR$ levels (Fig. 5 *A* and *B*). Quantification of receptor surface fluorescence showed a dramatic increase in Flz-conditioned neurons treated with leupeptin (control, 17,808 ± 1,954; Flz, 8,697 ± 891; Flz plus Leu, 16,359 ± 1,219). Leupeptin caused no significant changes in surface $GABA_AR$ cluster fluorescence for control neurons (control plus Leu, 17,447 ± 1,473). A similar rescue of $GABA_AR$ surface cluster area was observed (in μm^2): control, 0.30 ± 0.11; Flz, 0.17 ± 0.05; Con plus Leu, 0.29 ± 0.08; Flz plus Leu, 0.27 ± 0.08 (Fig. 5*C*). Analysis of α2-containing $GABA_AR$ cluster density showed a trend toward higher values with leupeptin treatment, although these did not reach statistical significance (expressed as % control: control, 101 ± 34; Flz, 60 ± 22; Con plus Leu, 138 ± 67; Flz plus Leu, 100 ± 41; $n = 8$–15 neurons from two to three independent cultures). Together, these data suggest that exposure of neurons to Flz results in enhanced lysosomal degradation of α2-subtype $GABA_ARs$ after their removal from the plasma membrane, reducing the total available $GABA_AR$ pool, decreasing inhibitory synapse size and number along with the efficacy of synaptic inhibition.

Discussion

We have begun to dissect the molecular mechanism underlying the neuronal adaptations in GABAergic inhibition induced by BZ treatment. We used live confocal imaging to identify subtype-specific changes in $GABA_AR$ neuronal surface levels and electrophysiology to measure BZ-dependent changes in inhibition. A

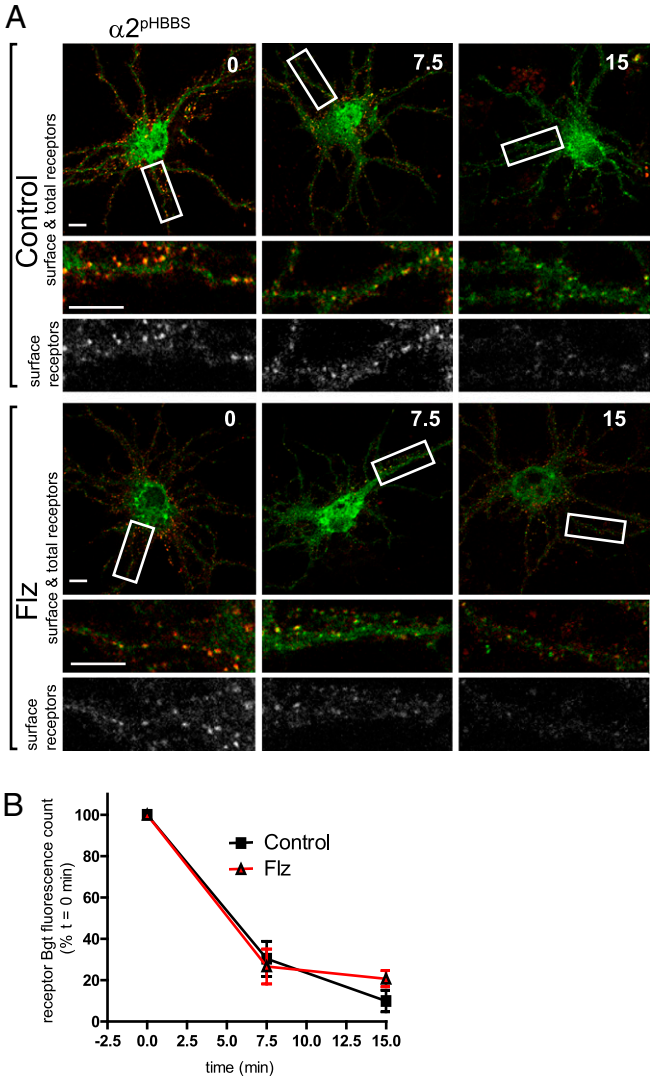

Fig. 4. $GABA_AR$ endocytosis rate is not increased by BZ treatment. (*A*) Confocal imaging of $GABA_AR$ endocytosis in control and Flz-treated neurons. Surface $GABA_AR$ in $\alpha2^{pHBBS}$ neurons were live-labeled with Alexa594::Bgt (red), and then unbound Alexa594::Bgt was removed by washing, followed by incubation at 37 °C. At $t = 0$, 7.5, and 15 min, samples were removed and fixed. Total receptor number was assayed by permeabilization and staining with anti-GFP antibody (green). Panels below are enlargements of boxed dendrites. (Scale bars, 10 μm.) (*B*) Graph represents the surface $GABA_AR$ Alexa594::Bgt fluorescence loss over time with endocytosis in control (Con) and Flz-treated neurons (normalized to the $t = 0$ Alexa594::Bgt surface signal for each treatment, respectively) (10–12 neurons per condition; $n = 3$ cultures; error bars represent ±SEM).

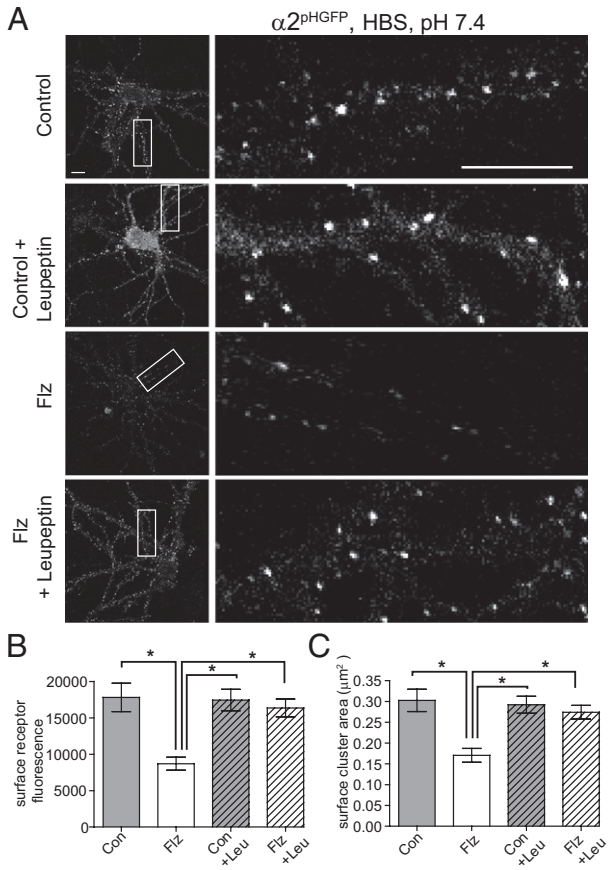

Fig. 5. $GABA_AR$ surface levels are restored in BZ-treated neurons by leupeptin treatment. (*A*) Live confocal imaging of neurons treated with or without 250 nM Flz for 24 h followed by control (Con) or 2-h 200 μM treatment with the lysosomal inhibitor leupeptin (Leu). (*Right*) Enlargements of boxed dendrites. (Scale bars, 10 μm.) (*B* and *C*) Mean ± SEM surface receptor $\alpha2^{pHGFP}$ fluorescence and cluster area [$^*P < 0.01$, one-way ANOVA (Bonferonni post test); 10–20 neurons per condition; $n = 3$ cultures].

comparison of α1- and α2-subtype $GABA_ARs$ showed α2-containing $GABA_AR$ surface levels were greatly diminished by 24-h BZ treatment. Further analysis showed that control neurons had nearly threefold higher total α2 levels compared with Flz-treated neurons. Concurrent with the decrease in $GABA_AR$ surface levels, Flz treatment resulted in a significant decrease in mIPSC amplitude. We demonstrated that the decrease in $GABA_AR$ surface levels occurs in a BZ binding site-dependent manner, as acute treatment with the BZ antagonist Ro 15-1788 restored the BZ-lowered $GABA_AR$ surface levels to control levels. Furthermore, acute Ro 15-1788 treatment returned mIPSC amplitude to control levels. Interestingly, BZ treatment did not alter the basal insertion and endocytosis rates of α2-containing $GABA_AR$. Rather, BZ treatment promoted the degradation of α2-containing $GABA_ARs$, decreasing the total available α2 $GABA_AR$ pool. Finally, blockade of lysosomal degradation was able to return α2 $GABA_AR$ surface levels in BZ-treated neurons to control levels. We anticipate that the sustained loss in surface and total $GABA_ARs$ during initial 24-h BZ treatment initiates a series of adaptations that develop into long-term changes in inhibition coincident with the development of BZ tolerance.

There is substantial evidence that a number of molecular processes are altered by short- and long-term BZ treatment, but comparatively little is understood regarding the initiation of these events. BZ treatment in vivo, in cultured neurons and in $GABA_AR$-transfected cell lines, leads to a reduction in the allosteric coupling of BZ and GABA binding sites (7), suggesting that homeostatic down-regulation occurs to diminish BZ-dependent enhancement of $GABA_AR$ activity. Although earlier experiments suggested that uncoupling manifested over several weeks, BZ allosteric uncoupling has been shown to occur after a single dose of diazepam, with peak attenuation occurring between 4 and 12 h and returning to normal after 24 h (21). This rapid uncoupling is consistent with reports in mammalian (22) and chick neuronal culture: Flz treatment of cultured chick neurons showed uncoupling of the BZ and GABA sites with a $t_{1/2}$ of ∼18 h (23). Combined with the rapid 24–48 h recovery from uncoupling both in animals chronically dosed or singly treated with BZ (21, 24), the current evidence suggests that BZs trigger an acute neuronal adaption modifying GABAergic inhibition. Studies of recombinant $GABA_AR$ expressed in Sf9 insect cells reported diazepam-induced uncoupling of both α1 (α1β2γ2) and α2 (α2β3γ2), with greater uncoupling of α2-containing receptors (25). This observation in a nonneuronal system suggests that individual subunits are uncoupled by distinct mechanisms, likely to be a posttranslational modification such as phosphorylation of $GABA_ARs$ or an interacting protein (26).

Importantly, many groups have shown that uncoupling occurs in vivo and in cultured systems without any contemporaneous changes in transcription or steady-state mRNA levels (21, 27, 28). These observations and reports of various, differing changes in mRNA levels (and often inverse changes in the same subunit) between different brain regions with chronic BZ treatment suggest that observed transcriptional changes may not directly correspond with functional changes in $GABA_AR$ protein levels, activity, and BZ tolerance (7). Although downstream signaling events after BZ administration are largely unknown, a recent microarray-based analysis following a single dose of diazepam identified a decrease in transcripts for CaMKIIα, BDNF, MKP-1, GIF, c-fos, and NGFI-A (29). Interestingly, the transcript levels had returned to baseline by 40 h for all of the genes except for CaMKIIα, further suggesting that key events may be posttranslational in nature.

Alterations in the regulated assembly, delivery, and removal of $GABA_ARs$ have been proposed as mechanisms for BZ treatment-induced changes of $GABA_AR$ activity, although they have not been thoroughly explored. Mice chronically treated with lorazepam show an increase in flunitrazepam binding in clathrin-coated vesicles and a decrease in synaptic membranes, suggesting sequestration of $GABA_ARs$ with BZ treatment (30). Studies of uncoupling in recombinant expression systems have also suggested BZ-induced internalization of $GABA_ARs$ into an acidic compartment that could retain BZ binding capability (26). Here, we show a mechanism for rapid neuronal adaptation to BZ treatment that occurs via enhanced degradation of α2-containing $GABA_ARs$, rather than alterations in receptor insertion or removal. The quick recovery of synaptic inhibition and $GABA_AR$ surface levels with 1 h of BZ antagonist Ro 15-1788 treatment is consistent with BZ-induced changes affecting receptor stability rather than protein synthesis. We surmise that the BZ antagonist Ro 15-1788 acts to restore $GABA_AR$ surface levels by blockade of BZ potentiation of GABA, thereby pushing GABAergic inhibition to low levels that are subsequently compensated for by increased $GABA_AR$ trafficking and reduced degradation.

Acute BZ tolerance has been reported with a single BZ dose (31–33), suggesting a link between rapid allosteric uncoupling and tolerance development. The underlying neuronal adaptations that modulate GABAergic signaling may be a highly evolutionarily conserved mechanism because treatment with the $GABA_A$ agonist muscimol in the nematode *Caenorhabditis elegans* results in selective removal of $GABA_AR$ from synapses during adaptation to muscimol, a process that occurs on a 24-h timescale and can largely be blocked in a mutant with defective lysosomal degradation (34). By providing a mechanism linking BZ treatment of neurons to changes in surface and total levels of $GABA_AR$ subtypes and the efficacy of neuronal inhibition, our results provide a mechanism for the initial

adaptations after BZ treatment. A greater understanding of these events and the subsequent long-lasting changes with chronic BZ treatment at an individual $GABA_AR$ subtype level will advance current treatment paradigms, potentially producing less tolerance and potential for abuse of one of the most widely prescribed medications in the Western world.

Materials and Methods

Cell Culture, Transfection, and Expression Constructs. Hippocampal neurons were prepared from embryonic day 18 rats, and constructs (14) were nucleofected at plating (Amaxa). The $\alpha2^{pHBBS}$ construct was generated by standard molecular biology techniques and sequenced. All studies were conducted in accordance with the institutional review boards of Tufts University School of Medicine and University of Pittsburgh School of Medicine.

Chemicals and Antibodies. Flz and Ro 15-1788 (Sigma) treatments were performed with 250 nM Flz and 5 μM Ro 15-1788. Anti-GFP antibodies were used as previously reported (13).

Live Imaging. Measurements were made on 14–17 d in vitro (DIV) hippocampal neurons at 37 °C in a closed heated chamber continuously perfused with extracellular Hepes-buffered saline, containing the following (in mM): 135 NaCl, 4.7 KCl, 10 Hepes, 11 glucose, 1.2 $MgCl_2$, and 2.5 $CaCl_2$ (adjusted to pH 7.4 with NaOH). Images were acquired using a Nikon A1 confocal microscope with a 60× oil objective (N.A., 1.4) at 2× zoom. Data were analyzed in Metamorph (Molecular Devices) as previously described (20), blind to experimental condition.

Insertion and Endocytosis Assays. Hippocampal neurons (14-17 DIV) expressing $\alpha2^{pHBBS}$ were assayed for $GABA_AR$ insertion (35) and endocytosis (20) with Bgt (Invitrogen) as previously and described in *Results*. All incubations were performed in the presence of 150 μM tubocurarine (Sigma) to block Bgt binding to endogenous acetylcholine receptors (36). See *SI Materials and Methods* for additional information.

Electrophysiology. Neurons were plated on 12-mm glass coverslips (German glass; VWR) coated with poly-L-lysine (0.5 mg/mL; Sigma) and cultured for 2–3 wk before the recordings. To measure mIPSCs, coverslips were placed in a recording chamber mounted on the stage of an inverted microscope and continually perfused with the following (in mM): 140 NaCl, 4.7 KCl, 10 Hepes, 11 glucose, 2 $MgCl_2$, and 2.5 $CaCl_2$ (adjusted to pH 7.4 with NaOH, 295–315 mOsm). For mIPSC recording, the extracellular solution was supplemented with 200 nM TTX, 10 μM CNQX, and 20 μM D-AP5 (Sigma). Borosilicate pipettes (3-6 MΩ) were filled with the following (in mM): 150 CsCl, 10 Hepes, 1.1 EGTA, 2 $MgCl_2$, 0.1 $CaCl_2$, 2 Mg^{2+}-ATP (adjusted to pH 7.2 with CsOH). Recordings were started 5–10 min after a stable whole-cell access was obtained. See *SI Materials and Methods* for additional information.

ACKNOWLEDGMENTS. The work was in part supported by National Institute of Neurological Disorders and Stroke Grants 046478, 048045, 051195, 056359, and NS054900. T.C.J. is in part supported by National Institute of Mental Health Grant R03 MH90253-01.

1. Poncer JC, Dürr R, Gähwiler BH, Thompson SM (1996) Modulation of synaptic $GABA_A$ receptor function by benzodiazepines in area CA3 of rat hippocampal slice cultures. *Neuropharmacology* 35(9–10):1169–1179.
2. Study RE, Barker JL (1981) Diazepam and (–)-pentobarbital: Fluctuation analysis reveals different mechanisms for potentiation of gamma-aminobutyric acid responses in cultured central neurons. *Proc Natl Acad Sci USA* 78(11):7180–7184.
3. Otis TS, Mody I (1992) Modulation of decay kinetics and frequency of $GABA_A$ receptor-mediated spontaneous inhibitory postsynaptic currents in hippocampal neurons. *Neuroscience* 49(1):13–32.
4. Sieghart W, Sperk G (2002) Subunit composition, distribution and function of $GABA_A$ receptor subtypes. *Curr Top Med Chem* 2(8):795–816.
5. Uusi-Oukari M, Korpi ER (2010) Regulation of $GABA_A$ receptor subunit expression by pharmacological agents. *Pharmacol Rev* 62(1):97–135.
6. Farrant M, Nusser Z (2005) Variations on an inhibitory theme: Phasic and tonic activation of $GABA_A$ receptors. *Nat Rev Neurosci* 6(3):215–229.
7. Bateson AN (2002) Basic pharmacologic mechanisms involved in benzodiazepine tolerance and withdrawal. *Curr Pharm Des* 8(1):5–21.
8. Poisbeau P, Williams SR, Mody I (1997) Silent $GABA_A$ synapses during flurazepam withdrawal are region-specific in the hippocampal formation. *J Neurosci* 17(10):3467–3475.
9. Zeng XJ, Tietz EI (1999) Benzodiazepine tolerance at GABAergic synapses on hippocampal CA1 pyramidal cells. *Synapse* 31(4):263–277.
10. Gallager DW, Lakoski JM, Gonsalves SF, Rauch SL (1984) Chronic benzodiazepine treatment decreases postsynaptic GABA sensitivity. *Nature* 308(5954):74–77.
11. Jacob TC, Moss SJ, Jurd R (2008) $GABA_A$ receptor trafficking and its role in the dynamic modulation of neuronal inhibition. *Nat Rev Neurosci* 9(5):331–343.
12. Kittler JT, et al. (2004) Huntingtin-associated protein 1 regulates inhibitory synaptic transmission by modulating gamma-aminobutyric acid type A receptor membrane trafficking. *Proc Natl Acad Sci USA* 101(34):12736–12741.
13. Saliba RS, Michels G, Jacob TC, Pangalos MN, Moss SJ (2007) Activity-dependent ubiquitination of $GABA_A$ receptors regulates their accumulation at synaptic sites. *J Neurosci* 27(48):13341–13351.
14. Tretter V, et al. (2008) The clustering of $GABA_A$ receptor subtypes at inhibitory synapses is facilitated via the direct binding of receptor alpha 2 subunits to gephyrin. *J Neurosci* 28(6):1356–1365.
15. Mukherjee J, et al. (2011) The residence time of $GABA_ARs$ at inhibitory synapses is determined by direct binding of the receptor α1 subunit to gephyrin. *J Neurosci* 31(41):14677–14687.
16. Mozrzymas JW, et al. (2007) GABA transient sets the susceptibility of mIPSCs to modulation by benzodiazepine receptor agonists in rat hippocampal neurons. *J Physiol* 585(Pt 1):29–46.
17. Rumpel E, Behrends JC (2000) Postsynaptic receptor occupancy during evoked transmission at striatal GABAergic synapses in vitro. *J Neurophysiol* 84(2):771–779.
18. Barnes EM, Jr. (1996) Use-dependent regulation of $GABA_A$ receptors. *Int Rev Neurobiol* 39:53–76.
19. Bogdanov Y, et al. (2006) Synaptic $GABA_A$ receptors are directly recruited from their extrasynaptic counterparts. *EMBO J* 25(18):4381–4389.
20. Jacob TC, et al. (2009) $GABA_A$ receptor membrane trafficking regulates spine maturity. *Proc Natl Acad Sci USA* 106(30):12500–12505.
21. Holt RA, Bateson AN, Martin IL (1999) Decreased GABA enhancement of benzodiazepine binding after a single dose of diazepam. *J Neurochem* 72(5):2219–2222.
22. Hu XJ, Ticku MK (1994) Chronic benzodiazepine agonist treatment produces functional uncoupling of the gamma-aminobutyric acid-benzodiazepine receptor ionophore complex in cortical neurons. *Mol Pharmacol* 45(4):618–625.
23. Roca DJ, Rozenberg I, Farrant M, Farb DH (1990) Chronic agonist exposure induces down-regulation and allosteric uncoupling of the gamma-aminobutyric acid/benzodiazepine receptor complex. *Mol Pharmacol* 37(1):37–43.
24. Tietz EI, Chiu TH, Rosenberg HC (1989) Regional GABA/benzodiazepine receptor/chloride channel coupling after acute and chronic benzodiazepine treatment. *Eur J Pharmacol* 167(1):57–65.
25. Primus RJ, et al. (1996) Allosteric uncoupling after chronic benzodiazepine exposure of recombinant gamma-aminobutyric acid(A) receptors expressed in Sf9 cells: Ligand efficacy and subtype selectivity. *J Pharmacol Exp Ther* 276(3):882–890.
26. Ali NJ, Olsen RW (2001) Chronic benzodiazepine treatment of cells expressing recombinant GABA(A) receptors uncouples allosteric binding: Studies on possible mechanisms. *J Neurochem* 79(5):1100–1108.
27. Wong G, Lyon T, Skolnick P (1994) Chronic exposure to benzodiazepine receptor ligands uncouples the gamma-aminobutyric acid type A receptor in WSS-1 cells. *Mol Pharmacol* 46(6):1056–1062.
28. Kang I, Miller LG (1991) Decreased $GABA_A$ receptor subunit mRNA concentrations following chronic lorazepam administration. *Br J Pharmacol* 103(2):1285–1287.
29. Huopaniemi L, Keist R, Randolph A, Certa U, Rudolph U (2004) Diazepam-induced adaptive plasticity revealed by alpha1 $GABA_A$ receptor-specific expression profiling. *J Neurochem* 88(5):1059–1067.
30. Tehrani MH, Barnes EM, Jr. (1997) Sequestration of gamma-aminobutyric $acid_A$ receptors on clathrin-coated vesicles during chronic benzodiazepine administration in vivo. *J Pharmacol Exp Ther* 283(1):384–390.
31. File SE, Wilks LJ, Mabbutt PS (1988) Withdrawal, tolerance and sensitization after a single dose of lorazepam. *Pharmacol Biochem Behav* 31(4):937–940.
32. Lister RG, Nutt DJ (1986) Mice and rats are sensitized to the proconvulsant action of a benzodiazepine-receptor inverse agonist (FG 7142) following a single dose of lorazepam. *Brain Res* 379(2):364–366.
33. Wong PT, Yoong YL, Gwee MC (1986) Acute tolerance to diazepam induced by benzodiazepines. *Clin Exp Pharmacol Physiol* 13(1):1–8.
34. Davis KM, et al. (2010) Regulated lysosomal trafficking as a mechanism for regulating $GABA_A$ receptor abundance at synapses in *Caenorhabditis elegans*. *Mol Cell Neurosci* 44(4):307–317.
35. Saliba RS, Pangalos M, Moss SJ (2008) The ubiquitin-like protein Plic-1 enhances the membrane insertion of $GABA_A$ receptors by increasing their stability within the endoplasmic reticulum. *J Biol Chem* 283(27):18538–18544.
36. Sekine-Aizawa Y, Huganir RL (2004) Imaging of receptor trafficking by using alpha-bungarotoxin-binding-site-tagged receptors. *Proc Natl Acad Sci USA* 101(49):17114–17119.